Research Article

Received: 9 November 2023 Revised: 26 February 2024 Accepted article published: 4 March 2024 Published online in Wiley Online Library: 12 March 2024

(wileyonlinelibrary.com) DOI 10.1002/ps.8055

Detection and coverage estimation of purple nutsedge in turf with image classification neural networks

Xiaojun Jin,[a,b] Kang Han,[b] Hua Zhao,[c] Yan Wang,[c] Yong Chen[a*] and Jialin Yu[b*]

Abstract

BACKGROUND: Accurate detection of weeds and estimation of their coverage is crucial for implementing precision herbicide applications. Deep learning (DL) techniques are typically used for weed detection and coverage estimation by analyzing information at the pixel or individual plant level, which requires a substantial amount of annotated data for training. This study aims to evaluate the effectiveness of using image-classification neural networks (NNs) for detecting and estimating weed coverage in bermudagrass turf.

RESULTS: Weed-detection NNs, including DenseNet, GoogLeNet and ResNet, exhibited high overall accuracy and F_1 scores (≥0.971) throughout the *k*-fold cross-validation. DenseNet outperformed GoogLeNet and ResNet with the highest overall accuracy and F_1 scores (0.977). Among the evaluated NNs, DenseNet showed the highest overall accuracy and F_1 scores (0.996) in the validation and testing data sets for estimating weed coverage. The inference speed of ResNet was similar to that of GoogLeNet but noticeably faster than DenseNet. ResNet was the most efficient and accurate deep convolution neural network for weed detection and coverage estimation.

CONCLUSION: These results demonstrated that the developed NNs could effectively detect weeds and estimate their coverage in bermudagrass turf, allowing calculation of the herbicide requirements for variable-rate herbicide applications. The proposed method can be employed in a machine vision-based autonomous site-specific spraying system of smart sprayers.

Keywords: deep learning; weed detection; weed-coverage estimation; precision herbicide application

1 INTRODUCTION

For centuries, turf has been an integrated part of the landscape, offering aesthetic, environmental and social benefits. It can be found in various settings, from residential yards to public parks.[1] Weeds are unwanted plants that grow on turf and compete with turfgrass for nutrients, water and sunlight, resulting in diminished visual appeal, impaired turf health and a depreciation in property value.[2,3] Herbicides are typically broadcast-applied uniformly across the entire field despite the patchy distribution nature of weeds.[4] This approach incurs high input costs and may pollute the environment.[5,6] In Europe, the cost of herbicides represents around 40% of the total expense for all chemicals used in agriculture.[7,8] Both economic and environmental concerns have led to legal regulations regarding herbicide usage in several countries.[9,10] For instance, the European Union introduced measures for reducing herbicide applications and encouraged spot-spraying in a dosage strictly necessary based on the degree of weed infestation.[7] Precision herbicide application refers to the intentional application of herbicides to specific areas where weeds are present, aiming to minimize herbicide usage and achieve effective weed control.[11,12] This approach can substantially reduce the environmental impact and economic cost associated with weed management.[13,14]

Precision herbicide application requires accurate weed detection and localization.[15–17] Image-processing techniques have been explored to detect and distinguish weeds by analyzing their visual characteristics, including color,[18,19] morphology[20] and texture.[21] Moreover, various studies have further expanded the application of machine vision methods for weed detection in turfgrasses. For example, Parra *et al*. implemented an edge-detection method to identify weeds in turfgrass.[22] They evaluated 12 edge-detection filters and the analysis revealed that sharpening filters combined with a minimum aggregation technique

* Correspondence to: Y Chen, College of Mechanical and Electronic Engineering, Nanjing Forestry University, Nanjing 210037, China. E-mail: chenyongjsnj@163.com (Chen) or J Yu, Peking University Institute of Advanced Agricultural Sciences/Shandong Laboratory of Advanced Agricultural Sciences at Weifang, Weifang 261325, China. E-mail: jialin.yu@pku-iaas.edu.cn (Yu)

a College of Mechanical and Electronic Engineering, Nanjing Forestry University, Nanjing, China

b Peking University Institute of Advanced Agricultural Sciences/Shandong Laboratory of Advanced Agricultural Sciences at Weifang, Weifang, China

c School of Mechanical Engineering, Jiangsu Ocean University, Lianyungang, China

yielded the most effective results. Ukrit *et al*. employed two weed-detection techniques, Bayes classifier and morphology operations, in turfgrass, achieving accuracies of 77.70–82.60% and 89.83–91.11%, respectively.[23] In another study, the methodology was enhanced by integrating texture and color features and employing a support vector machine in place of the Bayesian classifier, resulting in a significant improvement in weed-detection accuracy. The precision of the correct spray and spark rates reached 96.87% and 97.21%, respectively.[24] Nonetheless, these methods have limitations because crops and weeds may have similar morphological features.[2,25]

In recent years, deep learning (DL) techniques, particularly deep convolution neural networks (DCNNs), have shown remarkable progress in image classification, object detection and instance segmentation.[26,27] DCNNs can learn representations automatically from raw data, eliminating the need for handcrafted rules or human domain knowledge.[15,28] DL has been particularly effective in object detection, where it is used to identify and locate objects within an image.[28] This capability has been transformative for applications requiring precise visual recognition. Instance segmentation extends beyond detection by not only locating objects, but also delineating their boundaries at the pixel level, enabling detailed understanding of the scene, crucial for fields that demand high levels of accuracy in visual analysis.[29] Overall, the ability of DL models to learn complex representations from data has made them a powerful tool for a wide range of applications.[14] In agriculture, DL techniques have been widely applied in various aspects of modern agriculture, including crop yield prediction,[29,30] plant disease detection,[31,32] crop/weed classification[33,34] and livestock monitoring.[35,36] Nonetheless, implementing DL in agriculture, particularly for weed detection, has encountered obstacles because of the lack of abundant labeled data for supervised training. To address this issue, Hu *et al*. introduced a novel approach that combines image synthesis and semi-supervised learning (SSL) to train site-specific weed-detection models.[37] By utilizing 500 labeled images along with 1200 synthesized images for training and testing, this method enhanced the model's performance. Specifically, when trained with pseudo-labeled and synthetic images, the models exhibited a notable increase in mean average precision, with scores improving from 44.9 to 46.0 across three SSL iterations. These applications have shown great potential in increasing agricultural productivity, enhancing resource utilization and promoting sustainable development in the agricultural industry.[38]

Previous studies demonstrated the feasibility of using DCNNs for detecting and discriminating weeds growing in turf.[11,14,39,40] For example, Yu *et al*. reported that VGGNet achieved high F_1 scores (≥0.93) in detecting crabgrass (*Digitaria* spp.), dallisgrass (*Paspalum dilatatum* Poir.), doveweed [*Murdannia nudiflora* (L.) Brenan], and tropical signalgrass [*Urochloa distachya* (L.) T.Q. Nguyen] growing in bermudagrass turf.[40] Purple nutsedge (*Cyperus rotundus* L.) is known for its aggressive growth and resilience, making it a formidable weed in both ornamental and sports turf.[41] Several researchers have explored DL methods to effectively target this persistent species. Yu *et al*. compared five image-classification NNs—DenseNet, EfficientNet, ResNet, RegNet and VGGNet—to detect common dandelion (*Taraxacum officinale* Web.), dallisgrass, purple nutsedge and white clover (*Trifolium repens* L.) growing in bermudagrass turf, and found that VGGNet effectively detected and discriminated common dandelion, dallisgrass, purple nutsedge and white clover, whereas DenseNet, EfficientNetV2 and RegNet reliably detected and discriminated dallisgrass and purple nutsedge.[42] Chen *et al*. evaluated SSL methods to train image-classification NNs for detecting purple nutsedge and green kyllinga (*Kyllinga brevifolia*) in turfgrass.[43] The authors reported that networks utilizing the FixMatch SSL strategy and trained with input images of 240 × 240 pixels achieved the highest F_1 scores, reaching 98.1% with 100 labeled images and 98.2% with 200 labeled images.

Weed-coverage estimation is an essential input for implementing site-specific herbicide treatment, allowing for the calculation of herbicide requirements and the overall cost of weed management. Moreover, autonomous and accurate weed-coverage estimation could be used for variable-rate herbicide applications. At present, weed coverage is estimated by manual visual estimation. However, manual scouting of large fields is time-consuming and labor-intensive. Asad *et al*. employed maximum likelihood classification and DCNNs to detect weed density in canola (*Brassica napus* L.) fields.[44] The methodology involves segmenting foreground and background based on pixel values and manually labeling weed pixels. The labeled data are then used to train instance segmentation models to accurately estimate weed density. The ResNet-50-based SegNet model yielded the best results, with a mean intersection over a union (IoU) value of 0.8288 and a frequency-weighted IoU value of 0.9869. Mishra *et al*. utilized the Inception-v4 architecture, a DCNN, for detecting weed density in soybean (*Glycine max* L.) fields.[45] The weed density area is determined through vegetation segmentation.

DL techniques, such as image classification, object detection and instance segmentation NNs, are commonly employed in the domain of weed detection and discrimination.[38,46] Among these techniques, image classification involves the assignment of a predefined class label to an input image, focusing on the entire image without considering object-specific locations. Object detection, on the other hand, entails the identification of objects within an image, accompanied by placing bounding boxes and corresponding class labels. This approach effectively identifies multiple objects of varying classes, providing valuable location information. Instance segmentation aims to label each pixel within an image, resulting in segmentation of the image into distinct regions representing different object classes. Traditionally, weed-coverage estimation has necessitated pixel-level or individual plant-level analysis.[25] However, the inability of image classification to pinpoint object locations within an image renders it unsuitable for tasks demanding precise object positioning and pixel-level classification. Previous studies have predominantly relied on object detection and instance segmentation for weed-coverage estimation by analyzing pixel or individual plant-level information.[25] This methodology entails the classification of each image pixel as either a weed or a non-weed, requiring a substantial amount of annotated data for training, which can be both time-consuming and labor-intensive. Furthermore, the precision of the classification can be affected by variations in lighting and image quality, leading to potential misclassifications. A smart sprayer typically applies herbicides onto a specific spray zone rather than an individual pixel. This presents a challenge in translating the results obtained from pixel-level analysis to herbicide sprayers, because the pixel-based results are not directly applicable. To our knowledge, autonomous weed-coverage estimation in turf has not been previously reported. In the current research work, we proposed a novel integrated approach grounded in image-classification NNs for estimating weed coverage, extending the applicability of this approach beyond its established uses in the field. The objectives of this study were to: (i) evaluate the performance of image-classification NNs for detecting purple nutsedge growing in bermudagrass turf, and (ii) estimate its coverage in a grid framework for site-specific herbicide application.

2 MATERIALS AND METHODS

2.1 Overview

Three image-classification NNs, DenseNet,[47] GoogLeNet[48] and ResNet,[49] were selected to evaluate the feasibility of using image-classification NNs for detecting weeds growing in bermudagrass turf or estimating weed coverage in a grid framework to generate the herbicide application map. DenseNet (Dense Convolutional Network) is a DCNN that aims to address the vanishing gradient issue by employing feed-forward connections between each layer. This architecture enhances feature propagation and enables feature reuse through dense blocks, allowing DenseNet to achieve state-of-the-art accuracy with fewer parameters than other DL models. In addition, DenseNet is easy to implement and can be trained efficiently. GoogLeNet is a DL architecture developed by Google that introduced the concept of inception modules. These modules are made up of multiple layers with different filter sizes and stride lengths, which are combined in various ways to produce a rich set of features at different spatial resolutions. GoogLeNet also uses global average pooling and auxiliary classifiers to improve performance and reduce overfitting. The architecture has been shown to perform well on image-classification tasks, making it an efficient and practical choice for many applications. ResNet utilizes a novel design called residual blocks, which allows for the reuse of learned features and enables the training of very deep NNs. In a residual block, the input to a layer is added to the output of that layer after passing through a non-linear activation function. This creates a shortcut connection that enables the gradient signal to bypass one or more layers and flow directly to the earlier layers, thereby preventing the vanishing gradient issue. These image-classification NNs were utilized to detect weeds and estimate their coverage in bermudagrass turf. This approach extends the applicability of image classification beyond its established uses in the field, aiming to provide a more efficient and less resource-intensive solution.

2.2 Image acquisition

Images of purple nutsedge growing in bermudagrass turf were acquired in spring 2021 using a digital camera (Panasonic® DMC-ZS110, Xiamen, Fujian, China) with an original dimension of 2736×1824 pixels. The bermudagrass turf was naturally infested with purple nutsedge. The training images of purple nutsedge were captured at sod farms in Jiangning District, Nanjing, Jiangsu, China (31.95°N, 118.85°E), whereas the testing images were captured at sod farms in Shuyang, Jiangsu, China (34.12°N, 118.79°E). To increase the diversity of the training data set and improve the robustness of the DCNN, the training and testing images were captured at varying daytimes and weather conditions. All original images captured via the digital camera were cropped into grid cells to facilitate the tasks of weed detection and coverage estimation. Because of the limited presence of weeds in many original images, cropping the original images into grid cells results in only a small number of grid images containing weeds. Specifically, more than 600 original images were utilized to create a sufficient quantity of grid images containing weeds.

2.3 Training and testing

The image-classification NNs were trained and evaluated using the *k*-fold cross-validation methodology to ensure a comprehensive and thorough performance assessment. The data set was partitioned into five non-overlapping subsets in the *k*-fold cross-validation procedure (with $k = 5$ in this study). During each iteration, four subsets were utilized to train the image-classification NNs, whereas the remaining subset was used for validation. This process was repeated five times, with each subset serving as the validation data set exactly once. Through systematic rotation of the subsets, the NNs were thoroughly trained and assessed across diverse data configurations.

To constitute the training data set of the weed-detection NNs, images containing purple nutsedge growing in bermudagrass turf were cropped into 24 sub-images (4 rows $\times$ 6 columns, 24 grid cells) with a resolution of 456×456 pixels using a custom program developed with Python language (Fig. 1). A total of 8000 sub-images, with 4000 sub-images containing purple nutsedge growing in bermudagrass (true positive images) and 4000 sub-images containing bermudagrass only (true negative images), were divided into five distinct folds, resulting in each fold containing 1600 sub-images (800 images for each category). In every iteration, a training data set was created by amalgamating four subsets, resulting in a total of 6400 images. Simultaneously, the fifth subset (consisting of 1600 images) was reserved for validation. To constitute the testing data set of the weed-detection NNs, a total of 500 sub-images containing purple nutsedge growing in bermudagrass were randomly selected and used as the true positive images, whereas a total of 500 sub-images containing bermudagrass only were randomly selected and used as true negative images.

To constitute the training data set of the weed-coverage estimation NNs, images containing purple nutsedge growing in bermudagrass turf were cropped into 96 sub-images (8 rows $\times$ 12 columns, 96 grid cells) with a resolution of 228×228 pixels using a custom program developed with Python language (Fig. 1). A total of 8000 sub-images, with 4000 sub-images containing purple nutsedge growing in bermudagrass (true positive images) and 4000 sub-images containing bermudagrass only (true negative images), were divided into five distinct folds, resulting in each fold containing 1600 sub-images (800 images for each category). In every iteration, a training data set was created by amalgamating four subsets, resulting in a total of 6400 images. Simultaneously, the fifth subset (consisting of 1600 images) was reserved for validation. To constitute the testing data set of the weed-coverage estimation NNs, a total of 500 sub-images containing purple nutsedge growing in bermudagrass were randomly selected and used as the true positive images, whereas a total of 500 sub-images containing bermudagrass only were randomly selected and used as true negative images.

Moreover, additional experiments were conducted to train the image-classification NNs with the entire data set to fully substantiate the effectiveness of the proposed method. The aforementioned sub-images were combined and used as the training and testing data sets for weed-detection NNs and weed-coverage estimation NNs, respectively.

The image-classification NNs were trained and tested in PyTorch (version 1.8.1) open-source DL environment (Facebook, San Jose, CA, USA) with an NVIDIA GeForce RTX 2080 Ti graphic processing unit (NVIDIA; Santa Clara, CA, USA). Transfer learning is a machine-learning technique that leverages a pre-trained model as a

Figure 1. The originally captured image was cropped into 24 weed-detection cells (cyan lines) and 96 weed-coverage estimation cells (white lines).

foundation for training a new model on a related but different task. The pre-trained model typically learns from a vast and varied data set and captures general features beneficial for resolving various challenges. The image-classification NNs evaluated in this study were pre-trained using the ImageNet data set utilizing transfer learning to initialize the biases and weights.[50,51] The default hyperparameter values were utilized and implemented to ensure a fair comparison of the evaluated image-classification NNs (Table 1).

Precision, recall, overall accuracy and F_1 score are metrics commonly used to assess the efficacy of DL models. These metrics are calculated based on the elements of a confusion matrix. The binary classification confusion matrix contains four crucial elements, namely true positives (TP), true negatives (TN), false positives (FP) and false negatives (FN), which form the basis for evaluating the performance of image-classification NNs.

Precision measures the proportion of TP predictions made by the NN out of all the positive predictions. The calculation of precision involves the following equation[52]:

$$\text{Precision} = \frac{\text{TP}}{\text{TP} + \text{FP}} \quad (1)$$

Recall measures the proportion of true positive predictions made by the NN out of all actual positive cases in the data set. The calculation of recall involves the following equation[52]:

$$\text{Recall} = \frac{\text{TP}}{\text{TP} + \text{FN}} \quad (2)$$

Overall accuracy measures the proportion of correct predictions made by the NN over all predictions. The calculation of overall accuracy involves the following equation[52]:

TABLE 1. Hyperparameters used for training the image-classification neural networks

Deep learning architecture	Optimizer	Base learning rate	Learning rate policy	Batch size	Training epochs
DenseNet	SGD	0.001	LambdaLR	64	60
GoogLeNet	Adam	0.0003	StepLR	64	60
ResNet	Adam	0.0001	StepLR	64	60

Abbreviations: SGD, stochastic gradient descent.

$$\text{Overall accuracy} = \frac{TP+TN}{TP+FP+FN+TN} \tag{3}$$

The F_1 score is a composite metric that balances precision and recall. It is computed as the harmonic mean of these two measures, expressed as follows[52]:

$$F_1\ \text{score} = \frac{2 \times \text{precision} \times \text{recall}}{\text{precision} + \text{recall}} \tag{4}$$

Frames per second (FPS) is a measure of image processing algorithm speed that indicates the number of frames an algorithm can process per second. In the context of DL, a higher FPS corresponds to faster inference speeds for NNs.

2.4 Weed detection and coverage estimation

A custom software application was developed to incorporate OpenCV-Python (version 4.7.0.68) with the trained image-classification NNs for weed detection and coverage estimation in bermudagrass turf. The software generated grid cells on the input images and determined the presence of weeds in these grid cells. For weed detection, the custom software cropped each input image (2736 × 1824 pixels) to 24 equal-sized weed-detection cells (WDCs) with a resolution of 456 × 456 pixels. The trained weed-detection NNs were employed to detect and locate the WDCs containing weeds. The WDC was classified and marked as the spraying zone if the inference indicated it contained weeds.

After weed detection and localization, WDC containing weeds (the corresponding spraying zone) were further divided into four equal-sized weed-coverage estimation cells (WCECs) with a resolution of 228 × 228 pixels (2 rows × 2 columns). The trained weed-coverage estimation NNs were employed to detect the presence of weeds in each WCEC. The percentage of weed coverage was calculated based on the number of WCECs containing weeds: 25% (one of four cells contained weeds), 50% (two of four cells contained weeds), 75% (three of four cells contained weeds) and 100% (all four cells contained weeds). Figure 2 outlines the sequence diagram of weed detection and coverage estimation.

3 RESULTS

3.1 Performance of weed-detection NNs

3.1.1 *k-Fold cross-validation performance*

In this study, we employed the fivefold cross-validation methodology to rigorously assess the performance of the weed-detection NNs. The evaluation metrics, including precision, recall, overall accuracy and F_1 score, were computed across five different folds ($k1$ to $k5$) to ensure the robustness and reliability of our DL model's performance analysis.

No obvious differences were observed across all folds among the weed-detection NNs for detecting weeds growing in bermudagrass turf (Table 2). For discriminating the WDCs containing weeds with the cells containing bermudagrass turf exclusively, DenseNet and GoogLeNet had overall accuracy and F_1 score above 0.976 throughout the *k*-fold cross-validation. The performances of weed-detection NNs slightly declined in the testing data sets, but the overall accuracy and F_1 score never fell below 0.973. DenseNet outperformed GoogLeNet and ResNet with the highest overall accuracy and F_1 scores (≥0.980, $k3$/$k5$) in the validation and testing data sets.

3.1.2 *Performance evaluation trained on the entire data set*

There were no significant distinctions noted in the performance of various NNs for weed detection in bermudagrass turf, as illustrated in Table 3. For discriminating the WDCs containing weeds with the cells containing bermudagrass turf exclusively, all three NNs, DenseNet, GoogLeNet and ResNet, had overall accuracy and F_1 score above 0.976 in the validation data sets. The performances of weed-detection NNs slightly declined in the testing data sets, but the overall accuracy and F_1 score never fell below 0.972. DenseNet outperformed GoogLeNet and ResNet with the highest overall accuracy and F_1 scores (≥0.977) in the validation and testing data sets.

3.2 Performance of weed-coverage estimation NNs

3.2.1 *k-Fold cross-validation performance*

All weed-coverage estimation NNs exhibited excellent overall accuracy and F_1 scores with high precision and recall values across the entirety of the *k*-fold cross-validation (≥0.990) for discriminating the WCECs containing weeds and the cells containing bermudagrass turfgrass exclusively (Table 4). DenseNet, GoogLeNet and ResNet generally demonstrated similar performance levels on both the validation and testing data sets. The DenseNet weed-coverage estimation NNs showed the highest overall accuracy and F_1 scores in the validation and testing data sets (0.997, $k2$).

The stability of these metrics across different folds underscores the reliability and generalization capability of the NNs evaluated in this study. The consistently high precision, recall, overall accuracy and F_1 score values indicate that the trained NNs can effectively detect and discriminate grid cells containing the purple nutsedge and the bermudagrass turf. In conclusion, the results obtained from the *k*-fold cross-validation demonstrated the effectiveness and consistency of our DL models in the tasks of weed detection and coverage estimation.

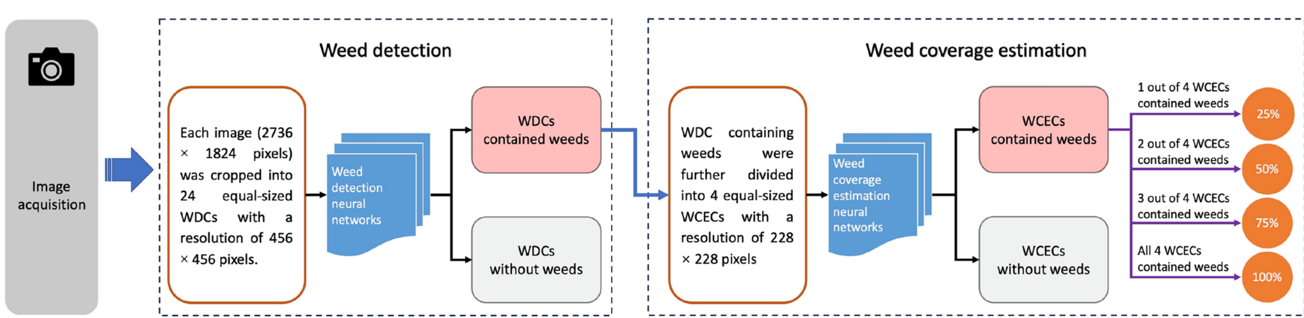

Figure 2. Flow diagram illustrating the sequence of weed detection and coverage estimation.

TABLE 2. *k*-Fold cross-validation performance metrics for weed-detection neural networks

Deep learning architecture	*k*-fold cross-validation	Label	Validation data set				Testing data set			
			Precision	Recall	Overall accuracy	F_1 score	Precision	Recall	Overall accuracy	F_1 score
DenseNet	*k*1	Turf	0.969	0.984	0.976	0.976	0.976	0.978	0.977	0.977
		Weed	0.984	0.969	0.976	0.976	0.977	0.976	0.977	0.976
	*k*2	Turf	0.966	0.994	0.979	0.980	0.967	0.990	0.978	0.978
		Weed	0.994	0.965	0.979	0.979	0.990	0.966	0.978	0.978
	*k*3	Turf	0.977	0.988	0.982	0.982	0.978	0.982	0.980	0.980
		Weed	0.987	0.976	0.982	0.981	0.982	0.978	0.980	0.980
	*k*4	Turf	0.967	0.990	0.978	0.978	0.969	0.985	0.977	0.977
		Weed	0.990	0.966	0.978	0.978	0.985	0.969	0.977	0.977
	*k*5	Turf	0.983	0.984	0.983	0.983	0.978	0.982	0.980	0.980
		Weed	0.984	0.982	0.983	0.983	0.982	0.978	0.980	0.980
GoogLeNet	*k*1	Turf	0.990	0.965	0.978	0.977	0.992	0.960	0.976	0.976
		Weed	0.966	0.990	0.978	0.978	0.961	0.992	0.976	0.976
	*k*2	Turf	0.966	0.996	0.981	0.981	0.967	0.990	0.978	0.978
		Weed	0.996	0.965	0.981	0.980	0.990	0.966	0.978	0.978
	*k*3	Turf	0.982	0.979	0.981	0.980	0.984	0.971	0.978	0.977
		Weed	0.979	0.982	0.981	0.980	0.972	0.984	0.978	0.978
	*k*4	Turf	0.979	0.982	0.981	0.980	0.979	0.980	0.979	0.979
		Weed	0.982	0.979	0.981	0.980	0.980	0.979	0.979	0.979
	*k*5	Turf	0.990	0.964	0.977	0.977	0.987	0.965	0.976	0.976
		Weed	0.965	0.990	0.977	0.977	0.966	0.988	0.976	0.977
ResNet	*k*1	Turf	0.953	0.991	0.971	0.972	0.959	0.989	0.973	0.974
		Weed	0.991	0.951	0.971	0.971	0.988	0.958	0.973	0.973
	*k*2	Turf	0.964	0.991	0.977	0.977	0.965	0.988	0.976	0.976
		Weed	0.991	0.962	0.977	0.976	0.987	0.964	0.976	0.975
	*k*3	Turf	0.964	0.994	0.978	0.979	0.962	0.994	0.978	0.978
		Weed	0.994	0.962	0.978	0.978	0.994	0.961	0.978	0.977
	*k*4	Turf	0.966	0.986	0.976	0.976	0.973	0.979	0.976	0.976
		Weed	0.986	0.965	0.976	0.975	0.979	0.972	0.976	0.975
	*k*5	Turf	0.974	0.990	0.982	0.982	0.974	0.984	0.979	0.979
		Weed	0.990	0.974	0.982	0.982	0.984	0.974	0.979	0.979

TABLE 3. Performance evaluation of weed-detection neural networks trained on the entire data set

Deep learning architecture	Label	Validation data set				Testing data set			
		Precision	Recall	Overall accuracy	F_1 score	Precision	Recall	Overall accuracy	F_1 score
DenseNet	Turf	0.980	0.986	0.983	0.983	0.974	0.980	0.977	0.977
	Weed	0.986	0.980	0.983	0.983	0.980	0.974	0.977	0.977
GoogLeNet	Turf	0.988	0.964	0.976	0.976	0.986	0.958	0.972	0.972
	Weed	0.965	0.988	0.976	0.976	0.959	0.986	0.972	0.972
ResNet	Turf	0.982	0.984	0.983	0.983	0.972	0.972	0.972	0.972
	Weed	0.984	0.982	0.983	0.983	0.972	0.972	0.972	0.972

3.2.2 *Performance evaluation trained on the entire data set*

In the validation data sets, NNs for estimating weed coverage achieved outstanding overall accuracy and F_1 scores (≥0.990), along with notable precision and recall values (Table 5). Across both validation and testing data sets, DenseNet, GoogLeNet and ResNet demonstrated comparable effectiveness for discriminating the WCECs containing weeds and the cells containing bermudagrass turfgrass exclusively. The DenseNet weed-coverage estimation NN showed the highest overall accuracy and F_1 scores at 0.996, followed closely by ResNet with scores of 0.994 in the testing data sets.

3.3 Weed mapping and coverage estimation

The results of weed detection and mapping using the custom software integrated with the weed-detection NNs are presented in Fig. 3. As mentioned in Section 3.2.2, each input image was

TABLE 4. *k*-Fold cross-validation performance metrics for weed-coverage estimation neural networks

Deep learning architecture	*k*-fold cross-validation	Label	Validation data set Precision	Validation data set Recall	Validation data set Overall accuracy	Validation data set F_1 score	Testing data set Precision	Testing data set Recall	Testing data set Overall accuracy	Testing data set F_1 score
DenseNet	*k*1	Turf	0.999	0.996	0.998	0.997	0.995	0.995	0.995	0.995
		Weed	0.996	0.999	0.998	0.997	0.995	0.995	0.995	0.995
	*k*2	Turf	0.996	1.000	0.998	0.998	0.995	0.999	0.997	0.997
		Weed	1.000	0.996	0.998	0.998	0.999	0.995	0.997	0.997
	*k*3	Turf	0.999	0.994	0.996	0.996	0.996	0.996	0.996	0.996
		Weed	0.994	0.999	0.996	0.996	0.996	0.996	0.996	0.996
	*k*4	Turf	0.997	0.994	0.996	0.995	0.995	0.998	0.996	0.996
		Weed	0.994	0.998	0.996	0.996	0.997	0.995	0.996	0.996
	*k*5	Turf	0.997	0.995	0.996	0.996	0.994	0.996	0.995	0.995
		Weed	0.995	0.998	0.996	0.996	0.996	0.994	0.995	0.995
GoogLeNet	*k*1	Turf	0.996	0.995	0.996	0.995	0.990	0.994	0.992	0.992
		Weed	0.995	0.996	0.996	0.995	0.994	0.990	0.992	0.992
	*k*2	Turf	0.991	0.995	0.993	0.993	0.991	0.994	0.992	0.992
		Weed	0.995	0.991	0.993	0.993	0.994	0.991	0.992	0.992
	*k*3	Turf	0.995	0.989	0.992	0.992	0.989	0.994	0.991	0.991
		Weed	0.989	0.995	0.992	0.992	0.994	0.989	0.991	0.991
	*k*4	Turf	0.988	0.992	0.990	0.990	0.986	0.994	0.990	0.990
		Weed	0.992	0.988	0.990	0.990	0.994	0.986	0.990	0.990
	*k*5	Turf	0.994	0.994	0.994	0.994	0.989	0.996	0.992	0.992
		Weed	0.994	0.994	0.994	0.994	0.996	0.989	0.992	0.992
ResNet	*k*1	Turf	0.998	0.998	0.998	0.998	0.996	0.996	0.996	0.996
		Weed	0.998	0.998	0.998	0.998	0.996	0.996	0.996	0.996
	*k*2	Turf	0.996	1.000	0.998	0.998	0.996	0.998	0.997	0.997
		Weed	1.000	0.996	0.998	0.998	0.997	0.996	0.997	0.996
	*k*3	Turf	0.997	0.995	0.996	0.996	0.995	0.996	0.996	0.995
		Weed	0.995	0.998	0.996	0.996	0.996	0.995	0.996	0.995
	*k*4	Turf	0.996	0.992	0.994	0.994	0.996	0.992	0.994	0.994
		Weed	0.993	0.996	0.994	0.994	0.993	0.996	0.994	0.994
	*k*5	Turf	0.994	0.998	0.996	0.996	0.990	1.000	0.995	0.995
		Weed	0.997	0.994	0.996	0.995	1.000	0.990	0.995	0.995

TABLE 5. Performance evaluation of weed-coverage estimation neural networks trained on the entire data set

Deep learning architecture	Label	Validation data set Precision	Validation data set Recall	Validation data set Overall accuracy	Validation data set F_1 score	Testing data set Precision	Testing data set Recall	Testing data set Overall accuracy	Testing data set F_1 score
DenseNet	Turf	0.998	0.994	0.996	0.996	0.996	0.996	0.996	0.996
	Weed	0.994	0.998	0.996	0.996	0.996	0.996	0.996	0.996
GoogLeNet	Turf	0.992	0.988	0.990	0.990	0.988	0.994	0.991	0.991
	Weed	0.988	0.992	0.990	0.990	0.994	0.988	0.991	0.991
ResNet	Turf	0.996	0.994	0.995	0.995	0.992	0.996	0.994	0.994
	Weed	0.994	0.996	0.995	0.995	0.996	0.992	0.994	0.994

divided into 24 WDCs. A total of 15 cells were identified as containing weeds and were marked with a red border; the remaining 8 cells exclusively contained bermudagrass turf.

Afterward, the exact WDCs on the input image containing weeds were further divided into four WCECs, as shown in Fig. 4. The trained weed-coverage estimation NNs were utilized to detect the presence or absence of weeds within each WCEC. As an example, in the WDC (spraying zone) located at the fourth column of the first row, two WCECs were detected to contain weeds, resulting in a weed-coverage percentage of 50% for this particular area (Fig. 5).

As shown in Fig. 5, the proposed method in this study effectively detected weeds and estimated their coverage growing in bermudagrass turf with the generation of weed-coverage mapping. A total of 3, 2, 6 and 4 of 15 spraying cells had a weed coverage of 25%, 50%, 75%, and 100%, respectively. Precision herbicide application can be achieved by directing the nozzle to the specific spraying cell where the weeds are present and adjusting the

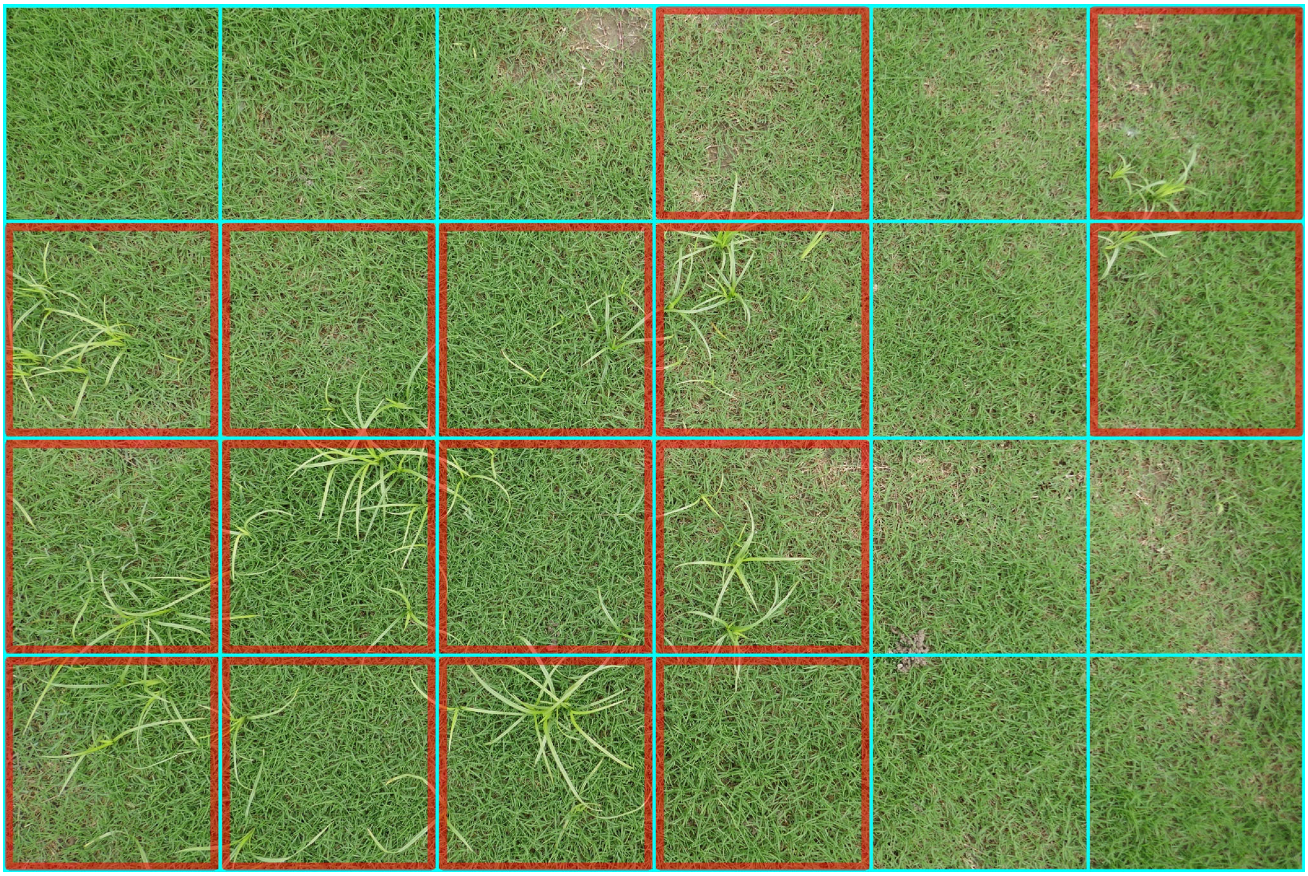

Figure 3. Weed-detection neural networks (NNs) successfully predicted the grid cells containing purple nutsedge while growing in bermudagrass (red borders) and bermudagrass only.

spraying volume based on the weed-coverage information obtained from our approach.

3.4 Inference speed of the image-classification NNs

The inference speed of the image-classification NNs is critical for real-time weed detection and coverage estimation. The FPS values of DenseNet, GoogLeNet and ResNet were computed by averaging the processing time of images from the testing data set. The WCECs are only created on the WDCs that contained weeds. Therefore, the theoretical minimum FPS occurs when all WDCs contain weeds, and all corresponding WCECs require processing by the weed-coverage estimation NN. In the current research effort, we calculated the theoretical minimum FPS by assuming that 24 WDCs contain weeds and thus require the processing of 96 corresponding WCECs. To calculate this value, the batch size of the weed detection and weed-coverage estimation NNs was set to 24 and 96, respectively, and the total inference time of the two NNs was measured (Table 6).

For weed-detection NNs, ResNet, with 87.62 sub-images (456×456 pixels) inferred per second, was 0.96 slower than GoogLeNet, but noticeably faster than DenseNet (51.20 FPS). For weed-coverage estimation NNs, ResNet and GoogLeNet, with 45.51 and 51.03 sub-images (228×228 pixels) inferred per second, demonstrated the fastest inference speed and outperformed DenseNet on computational efficiency. When considering the overall FPS values, GoogLeNet exhibited the highest FPS value of 33.33, whereas ResNet and DenseNet had speeds of 29.95 and 20 FPS, respectively. Based on a joint analysis of overall accuracy, F_1 score, and inference speed, ResNet demonstrated superior accuracy and computational efficiency compared with GoogLeNet and DenseNet. This competitive result may mainly come from its unique residual connections allowing deeper and more efficient NNs. Overall, these results suggested that ResNet was the most efficient and accurate CNN for turf weed detection and coverage estimation. Table 7 presents the overall FPS value for Fig. 3. As illustrated in Fig. 3, there are 15 WDCs containing weeds, resulting in the processing of 60 WCECs. Therefore, the batch size of the weed-coverage estimation model was set to 60, yielding an overall FPS value of 35.21 for ResNet. This value indicates that the ResNet can perform real-time weed detection and precision herbicide application with high accuracy.

4 DISCUSSION

In this study, each input image was divided into 24 equal-sized WDCs with a resolution of 456×456 pixels. The WDCs were classified and marked as spraying zones if the inference indicated they contained weeds. Implementing a subsequent decision-making system allows only the nozzles linked to those cells containing weeds to achieve precision herbicide spraying. In a practical machine vision system, the physical size of the WDCs should be equal to or slightly smaller than the area covered by a single nozzle. Therefore, careful consideration must be given to the size of the WDCs and the distribution of the nozzles to achieve optimal performance of the system and ensure effective precision herbicide application.

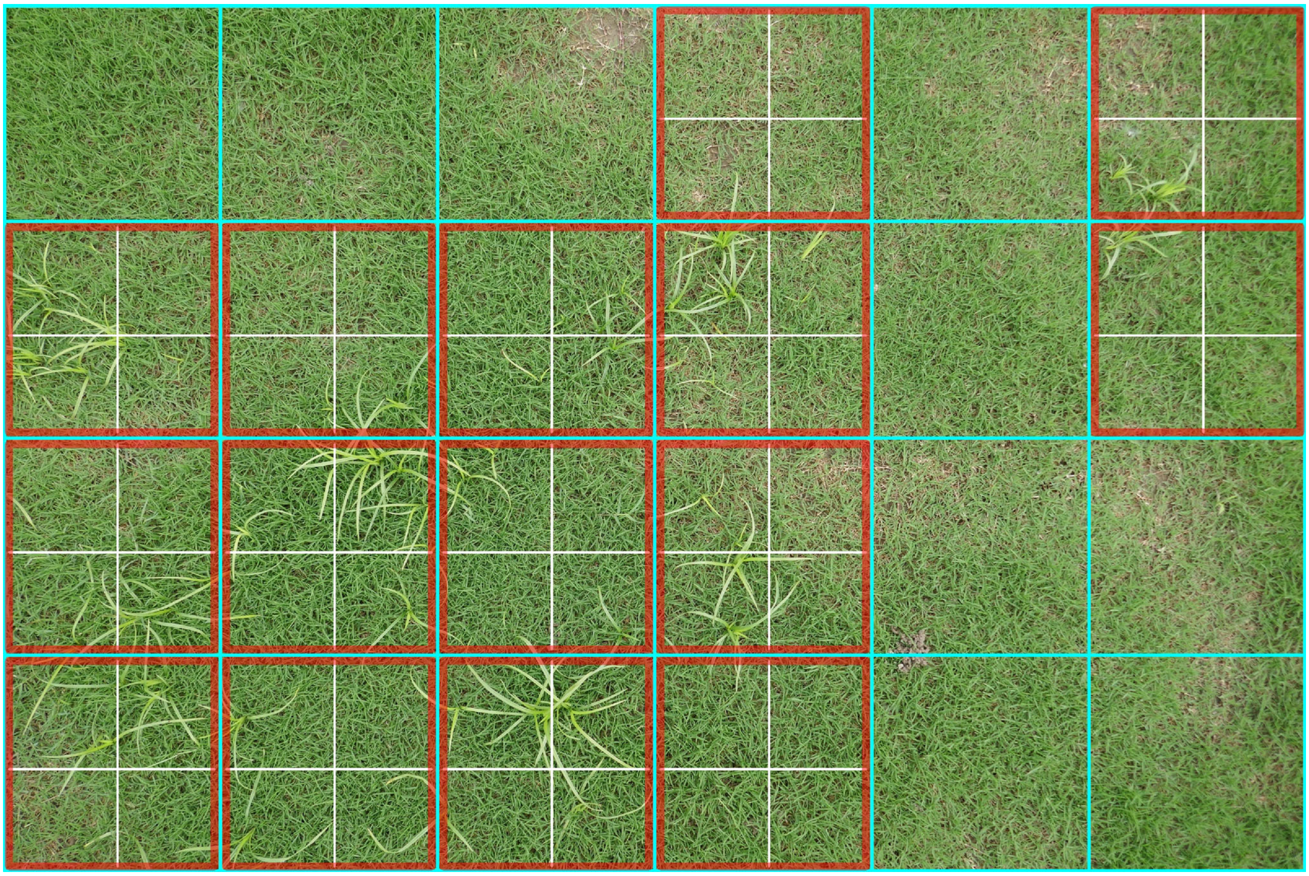

Figure 4. Each weed-detection cell containing weeds (spraying zone) was divided into four weed-coverage estimation cells.

Accurate detection of weeds and estimation of their coverage is crucial for implementing precision herbicide application, because it enables the calculation of herbicide requirements and the overall cost of weed control. In addition, weed-coverage estimation is necessary for carrying out variable-rate herbicide treatment. By accurately detecting the presence of weeds, the system can adjust the herbicide application rate according to the specific weed coverage in each WDC (spraying zone). In recent years, instance segmentation NNs have been extensively used for weed-coverage estimation by analyzing information at the pixel level.[44,45] This methodology involves the classification of every pixel in an image as either a weed or non-weed, requiring a substantial amount of annotated data for training. Moreover, in most cases, nozzles generate a specific size of spraying outputs, which presents a challenge in translating the results obtained from pixel-level analysis to herbicide sprayers. In this study, gird cells were generated on the input images, and image-classification NNs were utilized to detect whether the gird cells contained weeds. By utilizing this strategy, weed detection and coverage estimation can be achieved as long as the developed NNs can detect the presence or absence of weeds within each grid cell.

All three NNs, DenseNet, GoogLeNet and ResNet, exhibited high overall accuracy and F_1 scores (≥0.990) in the training and testing data sets when the NNs were trained with WCECs; however, these NNs exhibited reduced overall accuracy and F_1 scores when trained with WDCs. Therefore, it can be inferred that the training image size could affect the reliability of image-classification NNs for weed detection and coverage estimation. Similar trends were observed by Yang *et al.* who reported that increasing training image sizes from 200 × 200 pixels to 800 × 800 pixels reduced the weed-detection accuracy in Alfalfa (*Medicago sativa* L.) for all DL models evaluated in the study.[53] However, Zhuang *et al.* concluded that increasing the number of training images could enhance the performance of DCNNs while mitigating the impacts of training image sizes.[54] In this study, diminishing the size of the WCEC would lead to an elevated level of accuracy in estimating weed coverage. However, this enhancement comes at the expense of computational efficiency because it would require the classification of a larger number of grid images. Additional research is needed to investigate the implications of training image quantities and sizes on the performances of NNs for weed detection and coverage estimation in turf.

The need for high image processing speed is paramount to enable real-time weed detection and treatment. In automated weed control systems, actuators are constrained by the limited time available to process images and execute treatments.[55] Integrating these high-speed systems into robotic platforms facilitates real-time detection and action, even while the machinery is in motion. In this study, GoogLeNet and ResNet achieved notable speeds of 33.33 and 29.95 fps, respectively. These rates represent the theoretical minimum FPS for scenarios combining weed detection with coverage estimation tasks. The theoretical minimum FPS is calculated with the assumption that all WDCs contain weeds and all corresponding WCECs require processing by the

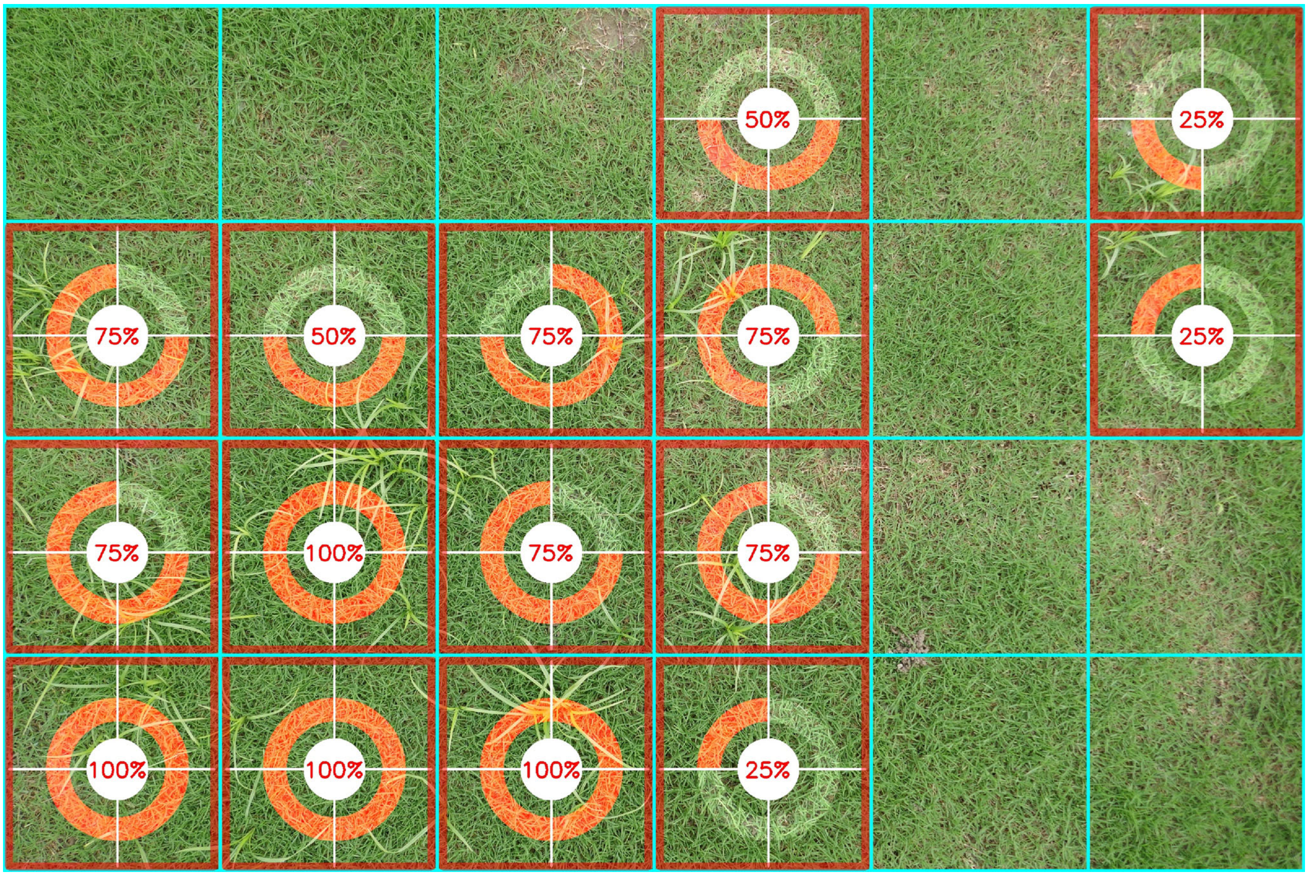

Figure 5. Results of weed mapping and coverage estimation. Weed-coverage percentage was classified into four levels (25%, 50%, 75%, and 100%) based on the number of weed-coverage estimation cells containing weeds.

TABLE 6. The inference time of the neural networks and minimum overall frames per second (FPS) of the full image

Deep learning architecture	Task	Full-image resolution	Sub-image resolution	Batch size	FPS	Overall FPS
DenseNet	Weed detection	2736 × 1824	456 × 456	24	51.20	20.00
	Weed-coverage estimation		228 × 228	96	32.35	
GoogLeNet	Weed detection		456 × 456	24	88.58	33.33
	Weed-coverage estimation		228 × 228	96	51.03	
ResNet	Weed detection		456 × 456	24	87.62	29.95
	Weed-coverage estimation		228 × 228	96	45.51	

TABLE 7. The inference time of the neural networks and the frames per second (FPS) of Fig. 3

Deep learning architecture	Task	Full-image resolution	Sub-image resolution	Batch size	FPS	Overall FPS
DenseNet	Weed detection	2736 × 1824	456 × 456	24	51.20	23.11
	Weed-coverage estimation		228 × 228	60	42.11	
GoogLeNet	Weed detection		456 × 456	24	88.58	37.79
	Weed-coverage estimation		228 × 228	60	65.90	
ResNet	Weed detection		456 × 456	24	87.62	35.21
	Weed-coverage estimation		228 × 228	60	58.88	

weed-coverage estimation NN. Weed control algorithms typically operate on embedded computers for deployment.[56] Although GoogLeNet and ResNet demonstrate potential for real-time weed detection and coverage estimation, it is critical to assess how these models perform under the constraints of such embedded systems, which warrants further investigation.

It is noteworthy that three classic image-classification NNs, DenseNet, GoogLeNet and ResNet, were used to validate the proposed methodology. The experimental results exhibited excellent outcomes, even using the classical DL models. These findings suggested the high feasibility of the weed detection and coverage estimation methods presented in this study. DL models come in a multitude of types and are evolving rapidly. We assume that employing state-of-the-art models will further enhance the accuracy of weed detection and coverage estimation, which warrants future investigation.

It should be noted that this study only evaluated purple nutsedge growing in bermudagrass turf for weed detection and coverage estimation. Although the weed detection and weed-coverage estimation NNs achieved high classification accuracy, a more diverse training data set that includes a broader range of weed species is highly desired. Expanding the NNs to have a greater variety of weed species would be the next step of this study. Such efforts would help to establish a more comprehensive and robust CNN that can effectively detect and estimate the coverage of diverse weed populations, thereby promoting precision herbicide applications.

5 CONCLUSIONS

This research demonstrated the feasibility and reliability of using image-classification NNs to detect weeds growing in bermudagrass turf and estimate their coverage in a grid framework, which will allow the calculation of herbicide requirements for site-specific and variable-rate herbicide applications. The developed weed-detection NNs can effectively detect and discriminate the grid cells containing the purple nutsedge and the bermudagrass turf, with overall accuracy and F_1 scores exceeding 0.972 in the testing data sets. The developed weed-estimation NNs can effectively detect and locate the grid cells containing weeds. Among the evaluated NNs, the DenseNet weed-coverage estimation NN showed the highest overall accuracy and F_1 scores (0.996). The inference speed of ResNet was similar to GoogLeNet, but noticeably faster than DenseNet. ResNet was the most efficient and accurate image-classification NN for weed detection and coverage estimation in turf. This is the first study attempting to detect and locate weeds and estimate their coverage using image-classification NNs. The proposed method can be employed in a machine vision system with an autonomous site-specific spraying system to achieve precision herbicide application.

ACKNOWLEDGEMENTS

This work was supported by the National Natural Science Foundation of China (Grant No. 32072498), the Taishan Scholars Program, and the Postgraduate Research & Practice Innovation Program of Jiangsu Province (Grant No. KYCX22_1051).

CONFLICT OF INTEREST

The authors declare no conflict of interest.

DATA AVAILABILITY STATEMENT

The data that support the findings of this study are available from the corresponding author upon reasonable request.

REFERENCES

1 Milesi C, Elvidge C, Dietz J, Tuttle B, Nemani R and Running S, A strategy for mapping and modeling the ecological effects of US lawns. *J Turfgrass Manage* **1**:83–97 (2005).
2 Hamuda E, Glavin M and Jones E, A survey of image processing techniques for plant extraction and segmentation in the field. *Comput Electron Agric* **125**:184–199 (2016).
3 Liu B and Bruch R, Weed detection for selective spraying: a review. *Curr Rob Rep* **1**:19–26 (2020).
4 McElroy J and Martins D, Use of herbicides on turfgrass. *Planta daninha* **31**:455–467 (2013).
5 Jin X, Bagavathiannan M, Maity A, Chen Y and Yu J, Deep learning for detecting herbicide weed control spectrum in turfgrass. *Plant Methods* **18**:94 (2022).
6 Fang S, Ru Y, Hu C, Yang F, Xue J and Zhou J, Planning the temporary takeoff/landing site's location for a pesticide spraying helicopter based on an intelligent fusion algorithm. *Comput Electron Agric* **209**:107826 (2023).
7 Peña JM, Torres-Sánchez J, de Castro AI, Kelly M and López-Granados F, Weed mapping in early-season maize fields using object-based analysis of unmanned aerial vehicle (UAV) images. *PloS One* **8**: e77151 (2013).
8 Jin X, Liu T, Yang Z, Xie J, Bagavathiannan M, Hong X *et al.*, Precision weed control using a smart sprayer in dormant bermudagrass turf. *Crop Prot* **172**:106302 (2023).
9 Jin X, Liu T, McCullough PE, Chen Y and Yu J, Evaluation of convolutional neural networks for herbicide susceptibility-based weed detection in turf. *Front Plant Sci* **14**:1096802 (2023).
10 Jin X, McCullough PE, Liu T, Yang D, Zhu W, Chen Y *et al.*, A smart sprayer for weed control in bermudagrass turf based on the herbicide weed control spectrum. *Crop Prot* **170**:106270 (2023).
11 Yu J, Schumann AW, Cao Z, Sharpe SM and Boyd NS, Weed detection in perennial ryegrass with deep learning convolutional neural network. *Front Plant Sci* **10**:1422 (2019).
12 Mennan H, Jabran K, Zandstra BH and Pala F, Non-chemical weed management in vegetables by using cover crops: a review. *Agronomy* **10**: 257 (2020).
13 Slaughter DC, Giles DK and Downey D, Autonomous robotic weed control systems: a review. *Comput Electron Agric* **61**:63–78 (2008).
14 Jin X, Liu T, Chen Y and Yu J, Deep learning-based weed detection in turf: a review. *Agronomy* **12**:3051 (2022).
15 Liakos KG, Busato P, Moshou D, Pearson S and Bochtis D, Machine learning in agriculture: a review. *Sensors* **18**:2674 (2018).
16 Fennimore SA, Slaughter DC, Siemens MC, Leon RG and Saber MN, Technology for automation of weed control in specialty crops. *Weed Technol* **30**:823–837 (2016).
17 Wang A, Zhang W and Wei X, A review on weed detection using ground-based machine vision and image processing techniques. *Comput Electron Agric* **158**:226–240 (2019).
18 Jin X, Che J and Chen Y, Weed identification using deep learning and image processing in vegetable plantation. *IEEE Access* **9**:10940–10950 (2021).
19 Tang J-L, Chen X-Q, Miao R-H and Wang D, Weed detection using image processing under different illumination for site-specific areas spraying. *Comput Electron Agric* **122**:103–111 (2016).
20 Perez A, Lopez F, Benlloch J and Christensen S, Colour and shape analysis techniques for weed detection in cereal fields. *Comput Electron Agric* **25**:197–212 (2000).
21 Bakhshipour A, Jafari A, Nassiri SM and Zare D, Weed segmentation using texture features extracted from wavelet sub-images. *Biosyst Eng* **157**:1–12 (2017).
22 Parra L, Marin J, Yousfi S, Rincón G, Mauri PV and Lloret J, Edge detection for weed recognition in lawns. *Comput Electron Agric* **176**: 105684 (2020).
23 Watchareeruetai U, Takeuchi Y, Matsumoto T, Kudo H and Ohnishi N, Computer vision based methods for detecting weeds in lawns. *Mach Vis Appl* **17**:287–296 (2006).
24 Watchareeruetai U, Takeuchi Y, Matsumoto T, Kudo H and Ohnishi N, Modified lawn weed detection: utilization of edge-color based SVM and grass-model based blob inspection filterbank, in *International Conference on Neural Information Processing*. Springer, Berlin, pp. 30–39 (2007).
25 Hasan AM, Sohel F, Diepeveen D, Laga H and Jones MG, A survey of deep learning techniques for weed detection from images. *Comput Electron Agric* **184**:106067 (2021).

26 Shi J, Li Z, Zhu T, Wang D and Ni C, Defect detection of industry wood veneer based on NAS and multi-channel mask R-CNN. *Sensors* **20**: 4398 (2020).
27 He T, Liu Y, Yu Y, Zhao Q and Hu Z, Application of deep convolutional neural network on feature extraction and detection of wood defects. *Measurement* **152**:107357 (2020).
28 Jordan MI and Mitchell TM, Machine learning: trends, perspectives, and prospects. *Science* **349**:255–260 (2015).
29 Nevavuori P, Narra N and Lipping T, Crop yield prediction with deep convolutional neural networks. *Comput Electron Agric* **163**:104859 (2019).
30 Khaki S and Wang L, Crop yield prediction using deep neural networks. *Front Plant Sci* **10**:621 (2019).
31 Lee SH, Goëau H, Bonnet P and Joly A, New perspectives on plant disease characterization based on deep learning. *Comput Electron Agric* **170**:105220 (2020).
32 Ferentinos KP, Deep learning models for plant disease detection and diagnosis. *Comput Electron Agric* **145**:311–318 (2018).
33 Jin X, Sun Y, Che J, Bagavathiannan M, Yu J and Chen Y, A novel deep learning-based method for detection of weeds in vegetables. *Pest Manag Sci* **78**:1861–1869 (2022).
34 Zhuang J, Jin X, Chen Y, Meng W, Wang Y, Yu J *et al*., Drought stress impact on the performance of deep convolutional neural networks for weed detection in Bahiagrass. *Grass Forage Sci* **78**:214–223 (2023).
35 Jung D-H, Kim NY, Moon SH, Jhin C, Kim H-J, Yang J-S *et al*., Deep learning-based cattle vocal classification model and real-time livestock monitoring system with noise filtering. *Animals* **11**:357 (2021).
36 Oliveira DAB, Pereira LGR, Bresolin T, Ferreira REP and Dorea JRR, A review of deep learning algorithms for computer vision systems in livestock. *Livest Sci* **253**:104700 (2021).
37 Hu C, Thomasson JA and Bagavathiannan MV, A powerful image synthesis and semi-supervised learning pipeline for site-specific weed detection. *Comput Electron Agric* **190**:106423 (2021).
38 Kamilaris A and Prenafeta-Boldú FX, Deep learning in agriculture: a survey. *Comput Electron Agric* **147**:70–90 (2018).
39 Xie S, Hu C, Bagavathiannan M and Song D, Toward Robotic Weed Control: Detection of Nutsedge Weed in Bermudagrass Turf Using Inaccurate and Insufficient Training Data *arXiv preprint arXiv:210608897* (2021).
40 Yu J, Schumann AW, Sharpe SM, Li X and Boyd NS, Detection of grassy weeds in bermudagrass with deep convolutional neural networks. *Weed Sci* **68**:545–552 (2020).
41 Small C, Degenhardt D, Drozdowski B, Thacker S, Powter C, Schoonmaker A *et al*., *Optimizing Weed Control for Progressive Reclamation: Literature Review*, Vol. **1**. InnoTech Alberta, Edmonton, AB, p. 48 (2018).
42 Jin X, Bagavathiannan M, McCullough PE, Chen Y and Yu J, A deep learning-based method for classification, detection, and localization of weeds in turfgrass. *Pest Manag Sci* **78**:4809–4821 (2022).
43 Chen X, Liu T, Han K, Jin X and Yu J, Semi-supervised learning for detection of sedges in sod farms. *Crop Prot* **179**:106626 (2024).
44 Asad MH and Bais A, Weed detection in canola fields using maximum likelihood classification and deep convolutional neural network. *Inf Process Agric* **7**:535–545 (2020).
45 Mishra AM, Harnal S, Gautam V, Tiwari R and Upadhyay S, Weed density estimation in soya bean crop using deep convolutional neural networks in smart agriculture. *J Plant Dis Prot* **129**:593–604 (2022).
46 dos Santos FA, Matte Freitas D, Gonçalves da Silva G, Pistori H and Theophilo Folhes M, Weed detection in soybean crops using ConvNets. *Comput Electron Agric* **143**:314–324 (2017).
47 Huang G, Liu Z, Van Der Maaten L and Weinberger KQ, Densely connected convolutional networks In *Proceedings of the IEEE conference on computer vision and pattern recognition*, pp. 4700–4708 (2017).
48 Szegedy C, Liu W, Jia Y, Sermanet P, Reed S, Anguelov D *et al*., Going deeper with convolutions In *Proceedings of the IEEE conference on computer vision and pattern recognition*, pp. 1–9 (2015.
49 He K, Zhang X, Ren S and Sun J, Deep residual learning for image recognition In *Proceedings of the IEEE conference on computer vision and pattern recognition*, pp. 770–778 (2016).
50 Lu J, Behbood V, Hao P, Zuo H, Xue S and Zhang G, Transfer learning using computational intelligence: a survey. *Knowl-Based Syst* **80**: 14–23 (2015).
51 Deng J, Dong W, Socher R, Li L-J, Li K and Fei-Fei L, Imagenet: A large-scale hierarchical image database In *2009 IEEE conference on computer vision and pattern recognition*. IEEE, pp. 248–255 (2009).
52 Sokolova M and Lapalme G, A systematic analysis of performance measures for classification tasks. *Inf Process Manag* **45**:427–437 (2009).
53 Yang J, Bagavathiannan M, Wang Y, Chen Y and Yu J, A comparative evaluation of convolutional neural networks, training image sizes, and deep learning optimizers for weed detection in Alfalfa. *Weed Technol* **36**:512–522 (2022).
54 Zhuang J, Li X, Bagavathiannan M, Jin X, Yang J, Meng W *et al*., Evaluation of different deep convolutional neural networks for detection of broadleaf weed seedlings in wheat. *Pest Manag Sci* **78**:521–529 (2022).
55 Sportelli M, Apolo-Apolo OE, Fontanelli M, Frasconi C, Raffaelli M, Peruzzi A *et al*., Evaluation of YOLO object detectors for weed detection in different turfgrass scenarios. *Appl Sci* **13**:8502 (2023).
56 Mwitta C, Rains GC and Prostko E, Evaluation of inference performance of deep learning models for real-time weed detection in an embedded computer. *Sensors* **24**:514 (2024).

